

Controllable optical output fields from an optomechanical system with a mechanical driving

Xun-Wei Xu¹ and Yong Li^{1,2,*}

¹Beijing Computational Science Research Center, Beijing 100084, China
²Synergetic Innovation Center of Quantum Information and Quantum Physics,
University of Science and Technology of China, Hefei, Anhui 230026, China

(Dated: January 28, 2022)

We investigate the properties of the optical output fields from a cavity optomechanical system, where the cavity is driven by a strong coupling and a weak probe optical fields and the mechanical resonator is driven by a coherent mechanical pump. When the frequency of the mechanical pump matches the frequency difference between the coupling and probe optical fields, due to the interference between the different optical components at the same frequency, we demonstrate that the large positive or negative group delay of the output field at the frequency of probe field can be achieved and tuned by adjusting the phase and amplitude of the mechanical driving field. Moreover, the strength of the output field at the frequency of optical four-wave-mixing (FWM) field also can be controlled (enhanced and suppressed) by tuning the phase and amplitude of the mechanical pump. We show that the power of the output field at the frequency of the optical FWM field can be suppressed to zero or enhanced so much that it can be comparable with and even larger than the power of the input probe optical field.

PACS numbers: 42.50.Wk, 42.50.Nn, 42.65.Dr, 42.65.Ky

I. INTRODUCTION

The field of optomechanical system that a movable mirror couples to a high-quality cavity via radiation pressure force has drawn much research attention in the past several years [1–4]. One of the motivations is that optomechanical system is an important candidate for signal transmission and storage. In analog to the optical responses in atomic system, a form of induced transparency called optomechanically induced transparency (OMIT) was pointed out theoretically [5]. Soon afterwards, the phenomenon of OMIT as well as optomechanically induced absorption and amplification was reported for observing in various optomechanical systems [6–15]. One important result concomitant with the modification of the optical response is a dramatic variation of the phase of the transmitted field and this will lead to a positive or negative group delay of the propagating field. Based on the OMIT, optomechanically induced absorption and amplification, optomechanical systems may be used for storage of optical signals [16–20], and the slowing, advancing and switch of optical pulses have been demonstrated experimentally [8, 12].

Moreover, if an optomechanical cavity is driven by a strong coupling field with frequency ω_c and a weak probe field with frequency ω_p , then, due to the optical radiation pressure, besides the fields at the applied field frequencies ω_c and ω_p , a optical four-wave-mixing (FWM) field with frequency $2\omega_c - \omega_p$ will be generated in the system. The FWM field induced by the radiation pressure in optomechanical systems has been investigated theoretically [21, 22], and it was shown that the strength of the FWM field can be enhanced by increasing the pump power of the strong coupling field. However, usually the power of the output FWM field is still much less than the power of the input probe field, and to our knowledge there is

no experimental report on the demonstration of FWM field in optomechanical systems to date.

Recently, the optical response properties in an optomechanical system with the mechanical resonator driven by an additional mechanical field was considered theoretically [23]. It was found in Ref. [23] that the optomechanically induced transparency, amplification or absorption for the probe field can be controlled by adjusting the phase and amplitude of the strong coupling field. In experiments, by applying both optical and mechanical driving fields to a multimode-cavity optomechanical system with both the optomechanical coupling and parametric phonon-phonon coupling [24], a cascaded optical transparency was observed and the extended optical delay and higher transmission as well as optical advancing were demonstrated.

Based on the optomechanical system with a mechanical pump [23, 24], in this paper we investigate in detail how to control the properties of the optical output fields from the cavity by adjusting the phase and amplitude of the mechanical pump. In the optomechanical system under consideration, the cavity is driven by a strong coupling optical field with frequency ω_c and a weak probe optical field with frequency ω_p , the mechanical resonator is driven by a coherent mechanical field with frequency ω_q . Due to the parametric coupling between the optical and mechanical modes, there are two kinds of optical components in the output field of the optomechanical system: the one induced by the strong coupling and weak probe optical fields with frequencies $\omega_c \pm m\delta$ ($\delta \equiv \omega_p - \omega_c$) and the one generated by the strong coupling optical field and the mechanical driving field (sidebands) with frequencies $\omega_c \pm n\omega_q$, where m and n are integers [25–27]. In particular, when the resonant condition $\omega_q = \delta \equiv \omega_p - \omega_c$ is fulfilled, the destructive or instructive quantum interference between these two kinds of optical output components provides us a way to control the properties of the optical fields output from an optomechanical system. For example, the optical delay of the output field at the frequency of optical probe field with fre-

*Electronic address: liyong@csrc.ac.cn

quency $\omega_p = \omega_c + \omega_q$ can be tuned accordingly by adjusting the phase and amplitude of the mechanical driving field. Moreover, the strength of the output field at the frequency of the FWM field $2\omega_c - \omega_p = \omega_c - \omega_q$ can also be controlled (i.e., enhanced and suppressed) by tuning the phase and amplitude of the mechanical driving field.

This paper is organized as follows: In Sec. II, we introduce the theoretical model of the optomechanical system with the driving of a strong coupling optical field, a weak probe optical field, and a mechanical pump. In Sec. III, the properties of the sidebands induced by parametric coupling in this optomechanical system is discussed. The effect of the mechanical driving field on the group delay of the output field at the frequency of probe optical field is investigated in Sec. IV. In Sec. V, the output field at the frequency of the FWM field with the presence of mechanical driving field is studied. We draw our conclusions in Sec. VI.

II. THEORETICAL MODEL

We consider an optomechanical system consisting of a single-sided optical cavity with a moving mirror (mechanical resonator) in the right-hand side [Fig. 1(a)]. The optical cavity is driven by a strong coupling field (amplitude ε_c , frequency ω_c) and a weak probe field (amplitude ε_p , frequency ω_p) from the left-hand side. A mechanical pump of strength $\Omega_m = 2\varepsilon_m \cos(\omega_q t + \phi_m)$ (amplitude ε_m , frequency ω_q , phase ϕ_m) is applied to the mechanical resonator via a tunable ac voltage source. In the rotating frame at the frequency of the optical coupling field ω_c , the Hamiltonian of the system is given by

$$\begin{aligned} H/\hbar = & \Delta_a a^\dagger a + \frac{1}{2} \omega_m (q^2 + p^2) + g a^\dagger a q \\ & + i (\varepsilon_c a^\dagger + \varepsilon_p e^{-i\delta t} e^{-i\phi_p} a^\dagger - \text{H.c.}) \\ & + 2q \varepsilon_m \cos(\omega_q t + \phi_m), \end{aligned} \quad (1)$$

where a (a^\dagger) denotes the bosonic annihilation (creation) operator of the cavity mode with resonance frequency ω_a in the absence of moving mirror; q and p are the dimensionless displacement and momentum operators of the moving mirror with resonance frequency ω_m . $\Delta_a = \omega_a - \omega_c$ ($\delta = \omega_p - \omega_c$) is the frequency detuning between the cavity mode (probe field) and the coupling field. We assume that ε_c and ε_p are real, and ϕ_p is the phase difference between the probe and coupling fields. This Hamiltonian (1) can also be realized by a micro-wheel cavity with optical mode coupling to a mechanical pinch mode through radiation pressure force [Fig. 1(b)] and the mechanical pinch mode is piezoelectrically driven by a radio frequency signal as in Ref. [24].

By the Heisenberg equations and the factorization assumption like $\langle qa \rangle = \langle q \rangle \langle a \rangle$, one gets the mean value equations for the operators of the optical and mechanical modes

$$\begin{aligned} \frac{d}{dt} \langle a \rangle = & -[\gamma_a + i(\Delta_a + g \langle q \rangle)] \langle a \rangle \\ & + \varepsilon_c + \varepsilon_p e^{-i\delta t} e^{-i\phi_p}, \end{aligned} \quad (2)$$

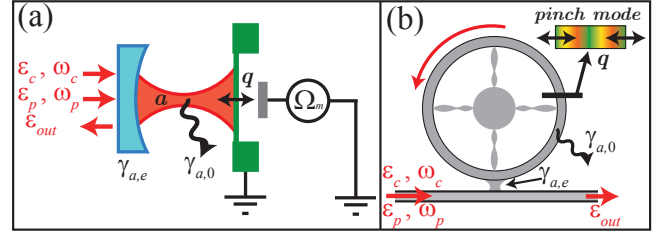


FIG. 1: (Color online) (a) Schematic of the optomechanical system for a Fabry-Perot optical cavity with a moving mirror (mechanical resonator). The optical cavity is driven by a coupling field and a probe field from the left-hand side. A mechanical pump Ω_m is applied to the mechanical resonator via an ac voltage source. (b) Experimental setup of the micro-wheel optomechanical system for optical mode coupling to a mechanical pinch mode through radiation pressure force, where the mechanical pump is realized by piezoelectric drive with radio frequency signal [24].

$$\begin{aligned} \frac{d^2}{dt^2} \langle q \rangle + \gamma_m \frac{d}{dt} \langle q \rangle + \omega_m^2 \langle q \rangle \\ = -\omega_m g \langle a^\dagger \rangle \langle a \rangle - 2\omega_m \varepsilon_m \cos(\omega_q t + \phi_m), \end{aligned} \quad (3)$$

where γ_m is the mechanical damping rate; $\gamma_a = \gamma_{a,0} + \gamma_{a,e}$ is the cavity damping rate, including the intrinsic loss $\gamma_{a,0}$ and the damping through the left-side mirror $\gamma_{a,e}$.

Firstly, we examine the mean values of the operators in the steady state and denote α_0 and q_0 the (zeroth-order) steady-state mean values for the cavity field and mechanical displacement when $\varepsilon_p \rightarrow 0$ and $\varepsilon_m \rightarrow 0$. The mean values in the steady state can be expressed as

$$\alpha_0 = \frac{\varepsilon_c}{\gamma_a + i\Delta}, \quad (4)$$

$$q_0 = -\frac{g}{\omega_m} |\alpha_0|^2, \quad (5)$$

where $\Delta = \Delta_a + gq_0$ is the effective detuning.

Generally, the mean values can be written as the sum of the steady state mean values and the time dependent ones, i.e., $\langle a \rangle = \alpha_0 + \tilde{\alpha}(t)$ and $\langle q \rangle = q_0 + \tilde{q}(t)$. Since the probe optical field and mechanical driving field are much weaker than the strong coupling optical field, i.e., $\{|\varepsilon_p|, |\varepsilon_m|\} \ll |\varepsilon_c|$, we have $|\alpha_0| \gg |\tilde{\alpha}(t)|$ and $|q_0| \gg |\tilde{q}(t)|$, then Eqs. (2) and (3) can be linearized by keeping the linear terms of the small time-dependent values,

$$\frac{d}{dt} \tilde{\alpha} = -(\gamma_a + i\Delta) \tilde{\alpha} - iG\tilde{q} + \varepsilon_p e^{-i\delta t} e^{-i\phi_p}, \quad (6)$$

$$\begin{aligned} \frac{d^2}{dt^2} \tilde{q} + \gamma_m \frac{d}{dt} \tilde{q} + \omega_m^2 \tilde{q} \\ = -\omega_m [\varepsilon_m e^{i(\omega_q t + \phi_m)} + G\tilde{\alpha}^* + \text{c.c.}], \end{aligned} \quad (7)$$

where $G = g\alpha_0$ is the effective optomechanical coupling rate.

With using the ansatz:

$$\tilde{\alpha} = \alpha_p e^{-i\delta t} + \alpha_p^* e^{i\delta t} + \alpha_m e^{-i\omega_q t} + \alpha_m^* e^{i\omega_q t}, \quad (8)$$

$$\tilde{q} = q_p e^{-i\delta t} + q_p^* e^{i\delta t} + q_m e^{-i\omega_q t} + q_m^* e^{i\omega_q t}, \quad (9)$$

one can obtain the solution of the coefficients as

$$\alpha_{p+} = \frac{\varepsilon_p e^{-i\phi_p}}{\gamma_a + i(\Delta - \delta) + i\chi(\delta) |G|^2}, \quad (10)$$

$$\alpha_{p-} = \frac{-iG}{\gamma_a + i(\Delta + \delta)} q_p^*, \quad (11)$$

$$q_p = \frac{\chi(\delta) G^* \varepsilon_p e^{-i\phi_p}}{\gamma_a + i(\Delta - \delta) + i\chi(\delta) |G|^2}, \quad (12)$$

$$\alpha_{m+} = \frac{-i\chi(\omega_q) G}{\gamma_a + i(\Delta - \omega_q) + i\chi(\omega_q) |G|^2} \varepsilon_m e^{-i\phi_m}, \quad (13)$$

$$\alpha_{m-} = \frac{-iG}{[\gamma_a + i(\Delta + \omega_q)]} q_m^*, \quad (14)$$

$$q_m = \frac{\chi(\omega_q) [\gamma_a + i(\Delta - \omega_q)]}{\gamma_a + i(\Delta - \omega_q) + i\chi(\omega_q) |G|^2} \varepsilon_m e^{-i\phi_m}, \quad (15)$$

where the mechanical effective susceptibility

$$\chi(\omega) = \frac{-\omega_m}{\left(\omega_m^2 - \omega^2 - i\gamma_m \omega + \frac{i\omega_m |G|^2}{\gamma_a - i(\Delta + \omega)} \right)}. \quad (16)$$

Note that in the right hand of Eq. (8), the first term means the optical probe field with frequency ω_p , the second terms represents the FWM field with frequency $2\omega_c - \omega_p \equiv \omega_p - 2\delta$, the third and fourth terms stand respectively for the (first) upper and lower sidebands generated by the strong coupling optical field and the mechanical driving field with frequencies $\omega_c \pm \omega_q$.

Using the input-output relation [28], the optical field output from the optomechanical cavity is given by

$$\varepsilon_{\text{out}} = 2\gamma_{a,e} \langle a \rangle - \varepsilon_c - \varepsilon_p e^{-i\delta t} e^{-i\phi_p}. \quad (17)$$

The output field at the frequency of the probe field (ω_p) is obtained as (normalized to the input power of the optical probe field)

$$t_p = \frac{2\gamma_{a,e} \alpha_{p+} - \varepsilon_p e^{-i\phi_p}}{\varepsilon_p e^{-i\phi_p}}, \quad (18)$$

and the FWM field (frequency $2\omega_c - \omega_p$) in the output of the cavity is given by

$$t_f = \frac{2\gamma_{a,e} \alpha_{p-}}{\varepsilon_p e^{-i\phi_p}}. \quad (19)$$

Besides, due to the mechanical driving field, there are two sidebands (t_u for the upper sideband $\omega_c + \omega_q$ and t_l for the lower sideband $\omega_c - \omega_q$) generated in the output field with the amplitudes

$$t_u = \frac{2\gamma_{a,e} \alpha_{m+}}{\varepsilon_m e^{-i\phi_m}}, \quad (20)$$

$$t_l = \frac{2\gamma_{a,e} \alpha_{m-}}{\varepsilon_m e^{-i\phi_m}}, \quad (21)$$

which are normalized to the power of the mechanical driving field.

If the frequency of the mechanical driving field is equal to the frequency detuning between the probe and coupling fields, i.e., $\omega_q = \delta \equiv \omega_p - \omega_c$, then the output field at the frequency of the probe field is obtained as (normalized to $\varepsilon_p e^{-i\phi_p}$)

$$t_{pu} = t_p + \eta t_u e^{i\phi}, \quad (22)$$

where $\eta = \varepsilon_m / \varepsilon_p$, $\phi = \phi_p - \phi_m$. The group delay τ_g is defined by [6, 8, 12]

$$\tau_g = \frac{d\theta}{d\delta}, \quad (23)$$

where $\theta = \arg(t_{pu})$ is the phase dispersion of the output field at the frequency $\omega_p = \omega_c + \omega_q$. The definition allows for a negative group delay ($\tau_g < 0$) which corresponds to the advancing of the probe field.

At the same resonant condition, the optical FWM field (with frequency $2\omega_c - \omega_p$) and the lower sideband (with frequency $\omega_c - \omega_q$) have the same frequency, then the output field at the frequency of the FWM field ($2\omega_c - \omega_p = \omega_c - \omega_q$) is given by (normalized to $\varepsilon_p e^{-i\phi_p}$)

$$t_{fl} = t_f + \eta t_l e^{i\phi}. \quad (24)$$

From Eqs. (22) and (24), the output fields are the coherent addition of the two parts (from the optical probe and the mechanical pump, t_p and ηt_u or t_f and ηt_l), and the relative amplitude η and phase difference between them ϕ can be used to control the properties of the output fields.

In the following sections, we will investigate the properties of the optical fields output from the optomechanical system numerically by the equations obtained in this section. In the numerical calculations, we use the parameters from a recent experiment [24]: $\omega_m = 2\pi \times 1.094$ GHz, $\gamma_a = 2\pi \times 0.255$ GHz, $\gamma_{a,e} = 0.2\gamma_a$ and $\gamma_m = 2\pi \times 16.8$ kHz. Without loss of generality, G is assumed real and positive in the following discussions. Here and afterwards, we fix $\Delta = \omega_m$, which provides the optomechanical cooling for the mechanical resonator and is widely applied in the previous works on OMIT [5–15].

III. MECHANICAL PUMP INDUCED SIDEBANDS

In this section, we will discuss about the sidebands induced by the mechanical pump given by Eqs. (20) and (21). Here, we only consider the first sidebands (upper sideband with the frequency $\omega_c + \omega_q$ and lower sideband with the frequency $\omega_c - \omega_q$) by taking the linear approximation in the derivation of Eqs. (20) and (21). The effect of higher-order sidebands can also be discussed by considering the nonlinear terms as in Ref. [27].

Figure 2 shows the strength of the output fields at the first-sideband ($|t_u|^2$ and $|t_l|^2$) as functions of the detuning $(\omega_q - \omega_m) / \gamma_m$ [panels (a) and (b)] and the optomechanical coupling rate $G / 2\pi$ [panels (c) and (d)]. There is a peak for the power spectrum of the output field at the first-sideband around the point $\omega_q = \omega_m$, and the linewidth of the spectrum

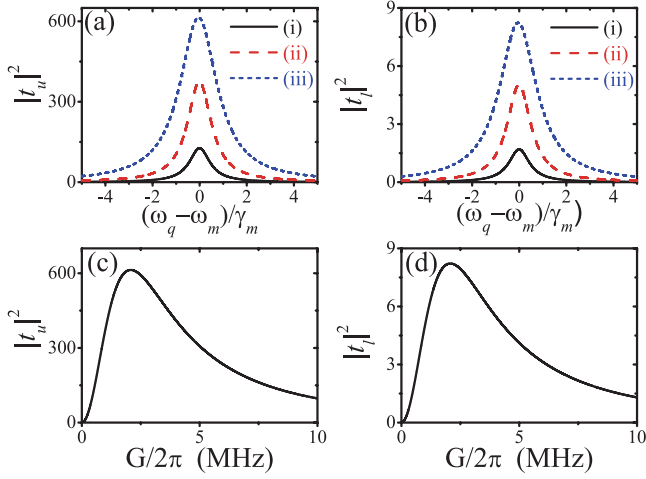


FIG. 2: (Color online) The strength of the output field at the upper sideband $|t_u|^2$ [(a) and (c)] and lower sideband $|t_l|^2$ [(b) and (d)] as functions of the detuning between mechanical mode and mechanical driving field [(a) and (b)] for optomechanical coupling rate taking different values [(i) $G = 2\pi \times 0.5$ MHz; (ii) $G = 2\pi \times 1.0$ MHz; (iii) $G = 2\pi \times 2.0$ MHz], and as functions of the optomechanical coupling rate [(c) and (d)] for mechanical resonator driven resonantly ($\omega_q = \omega_m$). Note that we fix $\delta = \omega_q$ and $\Delta = \omega_m$ here and afterwards. The other parameters are $\omega_m = 2\pi \times 1.094$ GHz, $\gamma_a = 2\pi \times 0.255$ GHz, $\gamma_{a,e} = 0.2\gamma_a$ and $\gamma_m = 2\pi \times 16.8$ kHz.

is broadened with the increase of the optomechanical coupling rate. Moreover, the strength of the output field at the first-sideband is much stronger than the mechanical driving field ($|t_u|^2 > 1$ and $|t_l|^2 > 1$) around the resonance point $\omega_q = \omega_m$, and the strength of the output field at the first-sideband is dependent on the strength of the optomechanical coupling rate.

As shown in Fig. 2(c) and 2(d), the strength of the output field at the first-sideband increases fast with the optomechanical coupling rate and reaches the maximum around $G = 2\pi \times 2.1$ MHz, which is consistent with the analytical result of the optimal value $G_{\text{om}} \simeq \sqrt{\gamma_a \gamma_m} = 2\pi \times 2.1$ MHz from Eqs. (11) and (18). As the increase of G above the optimal value G_{om} , the strength of the output field at the first-sideband decreases slowly with the optomechanical coupling rate because of the fast broadening of the spectrum when G becomes large.

IV. OPTICAL DELAY AND ADVANCING

As have been mentioned in the introduction, the optical response properties in an optomechanical system by coherently driving the mechanical resonator were investigated in Ref. [23], and optomechanically induced transparency, absorption and amplification are predicted for the probe field by adjusting the phase and amplitude of the coupling optical field. In addition to that, group delay is another important parameter to describe the optical responses. In this section, with Eqs. (22) and (23), we will show that the optical positive or negative group delay of the output field at the frequency

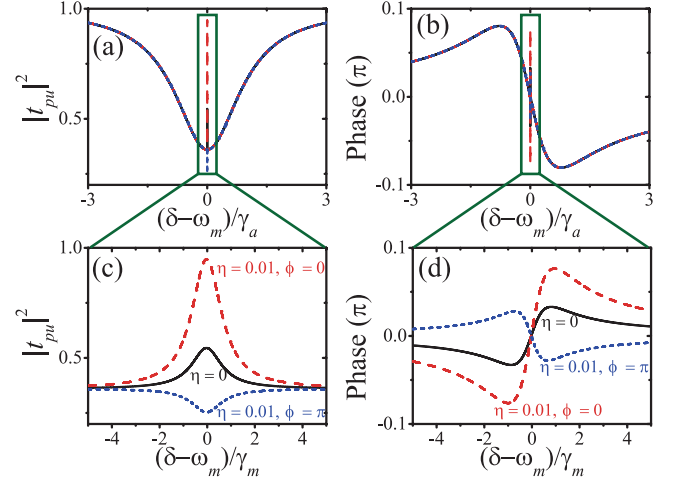


FIG. 3: (Color online) The output spectrum $|t_{pu}|^2$ [(a) and (c)] and phase [(b) and (d)] as functions of the detuning between probe and coupling fields. The black solid line is given for $\eta = 0$; the red dash line is given for $\eta = 0.01$ and $\phi = 0$; the blue short dash line is given for $\eta = 0.01$ and $\phi = \pi$. Here $G = 2\pi \times 1.5$ MHz. For the other parameters, see Fig. 2.

of optical probe field can be controlled by adjusting the phase and amplitude of the mechanical driving field.

The output spectrum $|t_{pu}|^2$ as a function of the detuning between the probe and coupling fields is presented in Fig. 3(a) and (c). In the case without the mechanical pump ($\eta = 0$), there is a low efficient transparency window with transmission rate $|t_{pu}|^2 \approx 0.54$ at $\delta = \omega_m$. When the mechanical pump is applied to the mechanical resonator with $\eta = 0.01$, the transparency of the probe field will be enhanced with transmission rate $|t_{pu}|^2 \approx 0.95$ for $\phi = 0$ or suppressed with transmission rate $|t_{pu}|^2 \approx 0.25$ for $\phi = \pi$. This is similar to that reported in Ref. [23]. In order to reveal more about the origin for the enhancing and suppressing of the output field induced by the mechanical pump, we show $|t_p|^2$, $|\eta t_u|^2$, and $|t_{pu}|^2$ as functions of the normalized amplitude of the mechanical pump η in Fig. 4. When $\phi = 0$, there is constructive interference between t_p and ηt_u , and one can find $|t_{pu}|^2 \simeq 4|t_p|^2 \simeq 4|\eta t_u|^2$ around $\eta = 0.031$ as shown in Fig. 4(a). When $\phi = \pi$, there is destructive interference between t_p and ηt_u , and one can find the strongest destructive interference $|t_{pu}|^2 \simeq 0$ around $\eta = 0.031$ as shown in Fig. 4(b).

The phase dispersion and the group delay of the output field at the frequency of the probe field are shown in Fig. 3(d) and Fig. 5(a), respectively. The enhancement of the optical transparency leads to faster variation of the phase [see the red dash line in Fig. 3(d)] and therefore larger optical group delay of the output field [see the red dash line in Fig. 5(a)]. Conversely, the suppression of the transparency induces negative derivative of the phase with respect to the frequency [see the blue short dash line in Fig. 3(d)] and negative group delay, that is the advancing of the output field [blue short dash line in Fig. 5(a)].

The effects of the mechanical pump on the group delay of the output field at the frequency of the probe field are shown in Fig. 5. From Fig. 5(a) and (b), the delay can be increased by

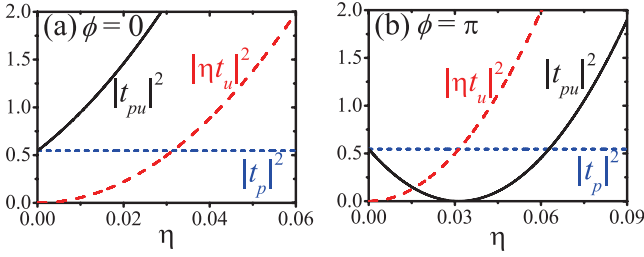


FIG. 4: (Color online) $|t_p|^2$, $|\eta t_u|^2$ and $|t_{pu}|^2$ plotted as functions of the normalized amplitude of the mechanical pump η for for $G = 2\pi \times 1.5$ MHz with (a) $\phi = 0$ and (b) $\phi = \pi$. Here $\delta = \omega_m$ and the other parameters are the same as in Fig. 2.

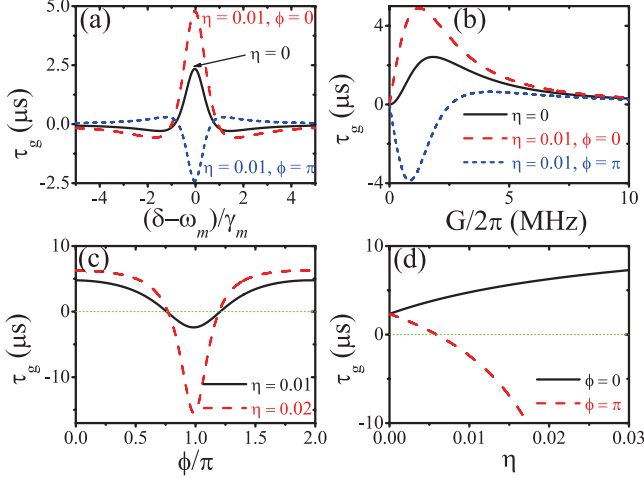


FIG. 5: (Color online) Group delay τ_g as a function of (a) the detuning between coupling and probe fields $(\delta - \omega_m)/\gamma_m$, (b) the effective optomechanical coupling rate G , (c) phase difference ϕ/π and (d) strength ratio η . In panels (b), (c) and (d), the detuning $\delta = \omega_m$. The other parameters are the same as in Fig. 2.

the mechanical pump ($\eta = 0.01$) with phase $\phi = 0$ or tuned to negative value when $\phi = \pi$. The group delay as a function of the amplitude η of the mechanical pump and phase ϕ is given in Fig. 5(c) and (d), and the tunable group delay (positive and negative) of the output field at the frequency of the probe field can be realized efficiently by adjusting the amplitude and phase of the mechanical pump.

The group delay as a function of the amplitude and phase of the mechanical pump is shown in Fig. 6(a). This plot shows that the group delay varies fast around the point $\eta \simeq 0.031$ and $\phi = \pi$, i.e., it can be tuned from the strong negative delay for η a little smaller than 0.031 to the strong positive delay for η a little larger than 0.031 at fixed $\phi = \pi$. This fast variation of group delay induced by the mechanical pump is associated with the changing from the absorption to the transparency of the probe field in the transmission spectrum as shown in Fig. 4(b). In addition, the group delay as a function of η for different values of the effective optomechanical coupling rate G is shown in Fig. 6(b). Much longer maximal possible delay (advancing) can be obtained for smaller G .

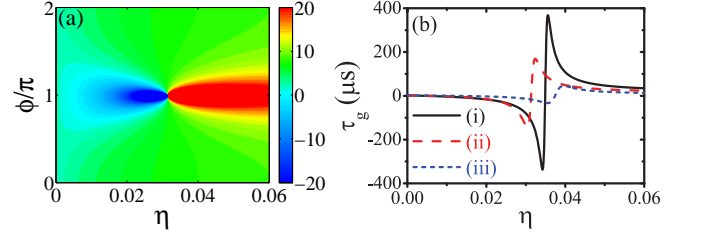


FIG. 6: (Color online) (a) Group delay τ_g (in units of μs) plotted as a function of η and ϕ/π for $G = 2\pi \times 1.5$ MHz. (b) τ_g plotted as a function of η for different values of G [(i) $G = 2\pi \times 1.0$ MHz; (ii) $G = 2\pi \times 1.5$ MHz; (iii) $G = 2\pi \times 3.0$ MHz] with $\phi = \pi$. In this figure, the detuning $\delta = \omega_m$ and the other parameters are the same as in Fig. 2.

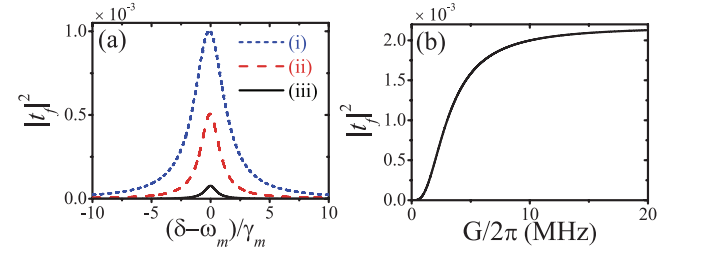


FIG. 7: (Color online) In the absence of mechanical pump $\eta = 0$, the normalized strength of the output FWM field $|t_f|^2$ plotted (a) as a function of the detuning $(\delta - \omega_m)/\gamma_m$ for different values of G [(i) $G = 2\pi \times 3$ MHz; (ii) $G = 2\pi \times 2$ MHz; (iii) $G = 2\pi \times 1$ MHz], and (b) as a function of G with $\delta = \omega_m$. The other parameters are the same as in Fig. 2.

V. CONTROL THE OUTPUT FIELD AT FREQUENCY OF FWM FIELD

The FWM field in standard optomechanical system has already been studied in some previous literatures [21, 22]. It was shown that the signal of FWM can be enhanced and exhibits normal-mode splitting as the increasing of the power of the coupling field (or the effective optomechanical coupling rate G) [21, 22]. The output FWM spectra in the absence of mechanical pump is shown in Fig. 7. There are two features for the FWM enhancement by the increase of G [21, 22]: (i) the linewidth of the FWM spectra is broadened with the strengthening of the FWM field; (ii) the strength of the FWM field will reach a saturation point [$|t_{fl}|_{\text{sat}}^2 \approx (\gamma_{a,e}/\omega_m)^2$] by the increase of G and the saturation strength is much smaller than the input probe field (about 2.2×10^{-3} for the parameters given in Fig. 7). In this section, with Eq. (24), we will show that the strength of the output field at the frequency of the FWM field also can be controlled by the mechanical pump.

In Fig. 8, the normalized strength of output field at the frequency of the FWM field $|t_{fl}|^2$ is plotted as a function of the detuning $(\delta - \omega_m)/\gamma_m$ for different values of the amplitude of the mechanical pump. When $\phi = 0$, with the strengthening of the mechanical pump, $|t_{fl}|^2$ increases significantly [Fig. 8(a)]. When $\phi = \pi$, with the strengthening of the mechanical pump, $|t_{fl}|^2$ are suppressed almost completely for

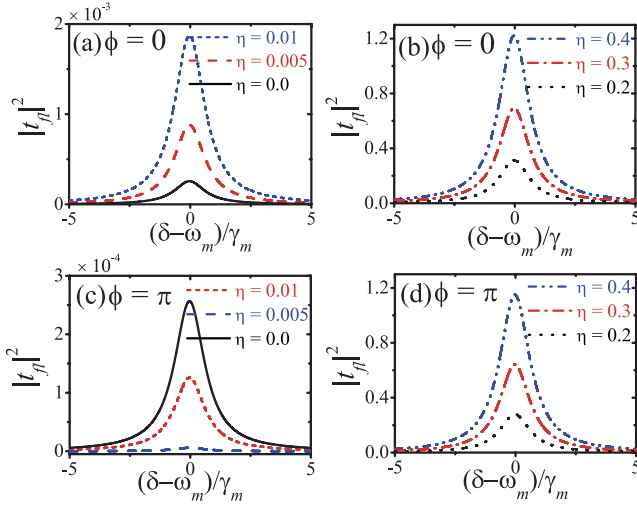


FIG. 8: (Color online) The normalized strength of the output field at the frequency of the FWM field $|t_{fl}|^2$ plotted as a function of the detuning $(\delta - \omega_m)/\gamma_m$ for different values of η with $\phi = 0$ in (a) and (b) and $\phi = \pi$ in (c) and (d). The other parameters are the same as in Fig. 2.

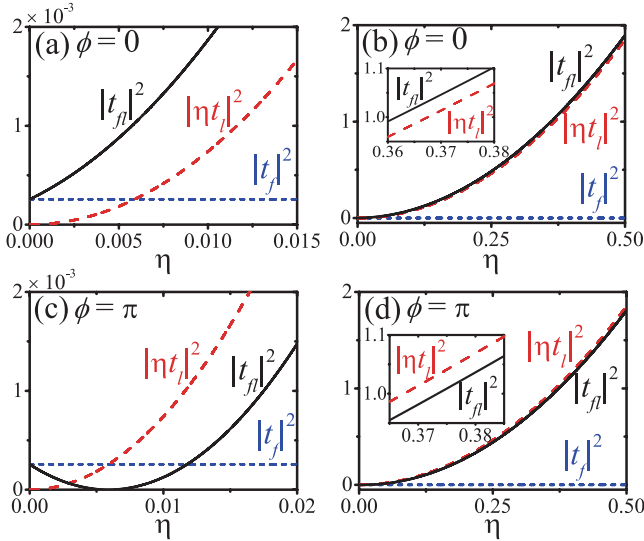


FIG. 9: (Color online) $|t_f|^2$, $|\eta t_l|^2$ and $|t_{fl}|^2$ plotted as functions of the normalized amplitude of the mechanical pump η with $\phi = 0$ in (a) and (b) and $\phi = \pi$ in (c) and (d). Here $\delta = \omega_m$ and $G = 2\pi \times 1.5$ MHz. The other parameters are the same as in Fig. 2.

$\eta = 0.005$ as shown in Fig. 8(c). $|t_{fl}|^2$ becomes comparable and even larger than the strength of input probe field with the further increase of η for both $\phi = 0$ and π as shown in Fig. 8(b) and (d). The linewidth of the output field at the frequency of the FWM field is almost fixed.

To explain the enhancing and suppressing of the strength of output field at the frequency of the FWM field induced by the mechanical pump, we show $|t_f|^2$, $|\eta t_l|^2$ and $|t_{fl}|^2$ as functions of the normalized amplitude of the mechanical pump η in Fig. 9. When $\phi = 0$, there is constructive interference between $|t_f|^2$ and $|\eta t_l|^2$, e.g., $|t_{fl}|^2 \simeq 4|t_f|^2 \simeq 4|\eta t_l|^2$ around

$\eta = 0.0059$ as shown in Fig. 9(a). When $\phi = \pi$, there is destructive interference between $|t_f|^2$ and $|\eta t_l|^2$, e.g., $|t_{fl}|^2 \simeq 0$ around $\eta = 0.0059$ as shown in Fig. 9(c). By further strengthening the mechanical pump, the strength of output field at the frequency of the FWM field increases monotonically with no saturation behavior, as shown in Fig. 9(b) and (d). The normalized strength of the output field at the frequency of the FWM field becomes larger than 1 when $\eta > 0.38$ and this mainly comes from the output field at the lower sideband induced by the mechanical pump.

Analytically, from Eq. (24), the output field at the frequency of the FWM field will vanish ($t_{fl} = 0$) at $\delta = \omega_m$ when the amplitude and phase for the mechanical pump satisfy

$$\eta e^{i\phi} = \frac{-G^*}{\gamma_a + i(\Delta - \delta)}. \quad (25)$$

With the parameters using in Fig. 9, that is, $G = 2\pi \times 1.5$ MHz, $\Delta = \delta = \omega_q = \omega_m$, and $\gamma_a = 2\pi \times 0.255$ GHz, one can find from Eq. (25) that the output field at the frequency of the FWM field will vanish ($t_{fl} = 0$) when $\eta \simeq 0.0059$ and $\phi = \pi$. This agrees well with the numerical result shown in Fig. 9(c).

VI. CONCLUSIONS

In summary, we have investigated the properties of the optical output fields from an optomechanical system in the presence of a strong coupling optical field, a weak probe optical field, and a mechanical pump. We demonstrate that the optical delay of the output field at the frequency of optical probe field can be tuned by adjusting the phase and amplitude of the mechanical driving field. This result may have potential applications in quantum information storage and transfer by realizing long optical delay or advancing in optomechanical systems. Moreover, the strength of the output field at the frequency of FWM field can also be controlled (enhanced and suppressed) by tuning the phase and amplitude of the mechanical driving field. The enhancing or suppressing of the output field at the frequency of FWM field is induced by the interference between the FWM field and the lower sideband field and it is worth mentioning that both of them are generated by the nonlinear processes. The efficient enhancing of the output field at the frequency of FWM field by a mechanical pump may provide a route to demonstrating FWM in the optomechanical systems experimentally.

Acknowledgement

We thank Q. Zheng for fruitful discussions. This work is supported by the Postdoctoral Science Foundation of China (under Grant No. 2014M550019), the National Natural Science Foundation of China (under Grants No. 11422437, No. 11174027, and No. 11121403) and the National Basic Research Program of China (under Grants No. 2012CB922104 and No. 2014CB921403).

-
- [1] T. J. Kippenberg and K. J. Vahala, *Science* **321**, 1172 (2008).
- [2] F. Marquardt and S. M. Girvin, *Physics* **2**, 40 (2009).
- [3] M. Aspelmeyer, P. Meystre, and K. Schwab, *Phys. Today* **65**, 29 (2012).
- [4] M. Aspelmeyer, T. J. Kippenberg, and F. Marquardt, *Rev. Mod. Phys.* **86**, 1391 (2014).
- [5] G. S. Agarwal and S. Huang, *Phys. Rev. A* **81**, 041803(R) (2010).
- [6] S. Weis, R. Rivière, S. Deléglise, E. Gavartin, O. Arcizet, A. Schliesser, and T. J. Kippenberg, *Science* **330**, 1520 (2010).
- [7] J. D. Teufel, D. Li, M. S. Allman, K. Cicak, A. J. Sirois, J. D. Whittaker, and R. W. Simmonds, *Nature (London)* **471**, 204 (2011).
- [8] A. H. Safavi-Naeini, T. P. M. Alegre, J. Chan, M. Eichenfield, M. Winger, Q. Lin, J. T. Hill, D. E. Chang, and O. Painter, *Nature (London)* **472**, 69 (2011).
- [9] F. Massel, T. T. Heikkilä, J. M. Pirkkalainen, S. U. Cho, H. Salmiemi, P. J. Hakonen, and M. A. Sillanpää, *Nature (London)* **480**, 351 (2011).
- [10] F. Massel, S. U. Cho, J. M. Pirkkalainen, P. J. Hakonen, T. T. Heikkilä, and M. A. Sillanpää, *Nat. Commun.* **3**, 987 (2012).
- [11] F. Hocke, X. Zhou, A. Schliesser, T. J. Kippenberg, H. Huebl, and R. Gross, *New J. Phys.* **14**, 123037 (2012).
- [12] X. Zhou, F. Hocke, A. Schliesser, A. Marx, H. Huebl, R. Gross and T. J. Kippenberg, *Nat. Phys.* **9**, 179 (2013).
- [13] M. Karuza, C. Biancofiore, M. Bawaj, C. Molinelli, M. Galassi, R. Natali, P. Tombesi, G. Di Giuseppe, and D. Vitali, *Phys. Rev. A* **88**, 013804 (2013).
- [14] V. Singh, S. J. Bosman, B. H. Schneider, Y. M. Blanter, A. Castellanos-Gomez, and G. A. Steele, *Nat. Nanotech.* **9**, 820 (2014).
- [15] K. Y. Fong, L. Fan, L. Jiang, X. Han, and H. X. Tang, *Phys. Rev. A* **90**, 051801(R) (2014).
- [16] C. Jiang, B. Chen and K. D. Zhu, *Europhys. Lett.* **94**, 38002 (2011).
- [17] B. Chen, C. Jiang, and K. D. Zhu, *Phys. Rev. A* **83**, 055803 (2011).
- [18] X. G. Zhan, L. G. Si, A. S. Zheng and X. Yang, *J. Phys. B: At. Mol. Opt. Phys.* **46**, 025501 (2013).
- [19] H. Wang, X. Gu, Y. X. Liu, A. Miranowicz, and F. Nori, *Phys. Rev. A* **90**, 023817 (2014).
- [20] H. Jing, S. K. Özdemir, Z. Geng, J. Zhang, X.-Y. Lü, B. Peng, L. Yang, and F. Nori, arXiv:1411.7115.
- [21] S. Huang and G. S. Agarwal, *Phys. Rev. A* **81**, 033830 (2010).
- [22] C. Jiang, B. Chen, and K. D. Zhu, *J. Opt. Soc. Am. B* **29**, 220 (2012).
- [23] W. Z. Jia, L. F. Wei, Y. Li, and Y.-x. Liu, *Phys. Rev. A* **91**, 043843 (2015).
- [24] L. Fan, K. Y. Fong, M. Poot, and H. X. Tang, *Nat. Commun.* **6**, 5850 (2015).
- [25] F. Marquardt, J. G. E. Harris, and S. M. Girvin, *Phys. Rev. Lett.* **96**, 103901 (2006).
- [26] A. Schliesser, R. Rivière, G. Anetsberger, O. Arcizet, and T. J. Kippenberg, *Nat. Phys.* **4**, 415 (2008).
- [27] H. Xiong, L. G. Si, A. S. Zheng, X. Yang, and Y. Wu, *Phys. Rev. A* **86**, 013815 (2012).
- [28] C. W. Gardiner and M. J. Collett, *Phys. Rev. A* **31**, 3761 (1985).